Journal of Colloid and Interface Science 326 (2008) 143–150

Contents lists available at ScienceDirect

Journal of Colloid and Interface Science

www.elsevier.com/locate/jcis

Detachment of colloids from a solid surface by a moving air–water interface

Prabhakar Sharma [a], Markus Flury [b,c,*], Jun Zhou [b]

[a] Section for Environmental Engineering, Aalborg University, Aalborg 9000, Denmark
[b] Department of Crop and Soil Sciences, Center for Multiphase Environmental Research, Washington State University, Pullman, WA 99164-6420, USA
[c] Department of Biological Systems Engineering, Washington State University, Pullman, WA, USA

ARTICLE INFO

Article history:
Received 11 April 2008
Accepted 13 July 2008
Available online 23 July 2008

Keywords:
Colloids
Detachment
Surface tension forces
Air–water interface

ABSTRACT

Colloid attachment to liquid–gas interfaces is an important process used in industrial applications to separate suspended colloids from the fluid phase. Moving gas bubbles can also be used to remove colloidal dust from surfaces. Similarly, moving liquid–gas interfaces lead to colloid mobilization in the natural subsurface environment, such as in soils and sediments. The objective of this study was to quantify the effect of moving air–water interfaces on the detachment of colloids deposited on an air-dried glass surface, as a function of colloidal properties and interface velocity. We selected four types of polystyrene colloids (positive and negative surface charge, hydrophilic and hydrophobic). The colloids were deposited on clean microscope glass slides using a flow-through deposition chamber. Air–water interfaces were passed over the colloid-deposited glass slides, and we varied the number of passages and the interface velocity. The amounts of colloids deposited on the glass slides were visualized using confocal laser scanning microscopy and quantified by image analysis. Our results showed that colloids attached under unfavorable conditions were removed in significantly greater amounts than those attached under favorable conditions. Hydrophobic colloids were detached more than hydrophilic colloids. The effect of the air–water interface on colloid removal was most pronounced for the first two passages of the air–water interface. Subsequent passages of air–water interfaces over the colloid-deposited glass slides did not cause significant additional colloid removal. Increasing interface velocity led to decreased colloid removal. The force balances, calculated from theory, supported the experimental findings, and highlight the dominance of detachment forces (surface tension forces) over the attachment forces (DLVO forces).

1. Introduction

Gas bubbles in a fluid can be used to remove particles from solid surfaces. When a gas bubble moves over a particle that is adhered to a solid surface, strong capillary forces form between the bubble and the particle, and the particle may detach from the adhering surface [1,2]. This principle is used in industrial applications, for instance to clean silicon wafers [3].

Various chemical and physical parameters affect the efficiency of gas bubbles to detach particles from a solid surface. Busscher and coworkers used a horizontal parallel-plate flow chamber to study detachment of Latex particles from uncoated and coated quartz or microscope glass slides [1,2,4,5]. They found that a moving liquid–air interface generates a very strong detachment force on adhered particles. The surface tension-based detachment force was several orders of magnitude larger than the adhesion force [1]. Particle detachment from surfaces by moving air-bubbles was more efficient for large liquid–air surface tensions and large particle sizes [2,4,5]. It was also observed that the more air-bubbles moved over a surface, the more particles were removed [2,4].

That gas bubbles form strong capillary forces with particles at the gas–liquid–solid interface is known from theory, and forces have experimentally measured by atomic force microscopy [6–8]. The detachment process caused by air-bubbles involves interception, thinning of the liquid film, film rupture, formation of a three-phase line, and stabilization of particle–bubble aggregates [2,9,10]. A particle can attach to an air-bubble only when the particle–bubble contact time is larger than the induction time, that is the necessary time to thin the liquid film and form the three-phase contact line [10]. The interaction force between a bubble and a particle is strongly dependent on the particle–bubble contact angle. This dependency is used in flotation to separate suspended particles, where hydrophobic particles are preferentially removed by attachment to liquid–gas interfaces in form of bubbles raising to the surface of a liquid [2,7,10,11].

* Corresponding author at: Department of Crop and Soil Sciences, Washington State University, Pullman, WA 99164-6420, USA. Fax: +1 509 335 8674.
E-mail address: flury@wsu.edu (M. Flury).

0021-9797/$ – see front matter
doi:10.1016/j.jcis.2008.07.030

Table 1
Selected properties of polystyrene colloids and suspension chemistry used in the experiments

Polystyrene colloids	Diameter[a] (μm)	Contact angle[b] (deg)	Surface charge[a] (meq/g)	Experimental conditions				
				$CaCl_2$ conc. (mM)	pH (–)	Electrophoretic mobility[c] (μm/s)/(V/cm)	ζ-potential[d] (mV)	Colloid conc. (particles/L)
Amidine-modified	1.0 ± 0.04	76.9 ± 1.8	0.0092	10	5.9	0.58 ± 0.12	7.4 ± 1.5	1.9×10^9
Amino-modified	1.0 ± 0.02	20.3 ± 1.9	0.1047	6	5.9	0.15 ± 0.02	1.9 ± 0.2	7.2×10^8
Carboxylate-modified	1.1 ± 0.04	19.5 ± 1.7	0.0175	10	4.3	-1.69 ± 0.03	-21.5 ± 0.4	2.7×10^9
Sulfate-modified	1.0 ± 0.03	104.9 ± 1.3	0.0017	10	4.3	-2.18 ± 0.17	-27.8 ± 2.1	3.6×10^9

[a] Values provided by manufacturer.
[b] Equilibrium contact angles measured with a goniometer (DSA 100, Krüss, Hamburg, Germany). The contact angle for the glass slide was $12.5 \pm 0.5°$.
[c] Measured with a ZetaSizer 3000HSa (Malvern Instruments Ltd., Malvern, UK) at the electrolyte concentration and pH indicated in the table.
[d] Obtained from measured electrophoretic mobilities using the von Smoluchowski equation [22]. The ζ-potentials for the glass slides were -32.5 ± 0.5, -33.4 ± 0.2, -33.3 ± 0.4, and -33.3 ± 0.4 mV for the solutions of the amidine, amino, carboxylate, and sulfate colloids, respectively.

Moving liquid–gas interfaces are also important for porous media flow and transport phenomena. It is likely that a moving liquid–gas interface can detach particles from porous media surfaces and carry particles along. In previous experiments, we have shown that a considerable amount of colloidal particles can be captured at the liquid–gas interface, and moved through a porous medium with an infiltration front [12]. Calculations using a numerical solution of the Young–Laplace equation have shown that subsurface colloids can be lifted from mineral surfaces by expanding water films [13]. From microscopic visualization using transparent micromodels, it is known that colloids can attach to the liquid–gas interfaces during transport through porous media [14,15]. Sirivithayapakorn and Keller [16] observed that colloids (Latex particles) attach to the air–water interface and move with them, and colloids formed clusters when air-bubbles dissolved.

The effects of moving air-bubbles on the detachment of submicron-sized particles (usually Latex particles) from initially wet solid surfaces have been investigated under different physical and chemical conditions [1–5]. However, the effects of moving liquid–gas interfaces over initially dry surfaces have not yet been investigated. The movement of liquid–gas interfaces over initially dry surfaces occurs frequently in natural unsaturated porous media (e.g., the vadose zone), when water infiltrates or imbibes dry soil or sediments. In this work, we examined the detachment of colloids, attached to a solid surface under initially air-dry conditions, when the surface is wetted and a liquid–gas interface is moved over the colloids.

Our main objective was to study the effect of moving liquid–gas interfaces on detachment of colloidal particles from an air-dry solid surface. We hypothesized that hydrophobic colloids are more easily removed than hydrophilic colloids by a liquid–gas interface. We further hypothesized that more colloids detach from the solid surface when colloids are attached under unfavorable as compared to favorable conditions. We deposited hydrophilic and hydrophobic colloids under favorable and unfavorable conditions onto glass slides and quantified colloid detachment after passages of air–water interfaces as a function of number of passages and interfacial velocities. Experimental data were then compared with theoretical force calculations.

2. Materials and methods

2.1. Colloids

We selected four different types of polystyrene colloids for the experiments: hydrophobic amidine-modified, hydrophilic amino-modified, hydrophilic carboxylate-modified, and hydrophobic sulfate-modified microspheres (Molecular Probes Inc., Eugene, OR). The carboxylate-modified and sulfate-modified microspheres were negatively charged while the amidine-modified and amino-modified microspheres were positively charged. All four colloids were fluorescent with an excitation wavelength of 505 nm and an emission wavelength of 515 nm (yellow-green). The specific density of all four colloids, according to the manufacturer, was 1.055 g/cm^3. The air–water contact angles of the colloids were measured by the sessile drop method with a goniometer (DSA 100, Krüss, Hamburg, Germany). Properties of the colloids are listed in Table 1.

2.2. Suspension chemistry

We intended to deposit colloids under both favorable and unfavorable conditions onto microscope glass slides. Colloid deposition is favorable in the absence of repulsive interaction, i.e., surface charges are opposite for glass slide and colloids, whereas unfavorable in the presence of repulsive interaction, i.e., similar surface charges. For that purpose, we first determined electrophoretic mobilities and ζ-potentials at different pH and ionic strengths for each of the colloids and glass slides. We then selected those solutions in which the colloids did not aggregate in solution and also did not form aggregates on the glass slides after air drying. For example, amino-modified colloids formed aggregates up to 6-layers thick during the deposition process on the glass slide at pH 4.1 and a $CaCl_2$ concentration of 0.5 mM, but formed single-particle depositions on the glass slides at pH 5.9 and 6 mM $CaCl_2$. Based on Derjaguin–Landau–Verwey–Overbeek (DLVO) calculations using measured ζ-potentials and ionic strengths, we chose appropriate solution conditions, such that favorable and unfavorable attachment conditions were obtained. The final experimental conditions chosen are shown in Table 1.

2.3. Deposition surface and deposition chamber

A flow chamber, an open flat channel made of Plexiglas, was used to deposit the colloids on a glass microscope slide (7.5 cm × 2.5 cm) (frosted microscope slides, pre-cleaned, Fisher Scientific). The channel was rectangular in shape with a dimension of 16 cm × 2.7 cm × 1 cm without a top cover. Both sides of the channel were connected (length wise) with Tygon tubing, and a peristaltic pump (Ismatec IP4, Glattburg, Switzerland) was used to supply solution from an inflow bottle to the inlet port and to suck the solution out of the channel from the outlet port. For colloid deposition, the channel was filled with a specific colloid suspension (Table 1) and recirculated. The flow rate in the channel was 50 mL/h. A microscope slide was then placed into the flow chamber, and submerged into the suspension. The colloid suspension was recirculated for four hours to deposit colloids onto the microscope slide. Then, the inflow was switched to a colloid-free solution having the same solution chemistry as the colloid suspension for another four hours to rinse the slide free of unattached colloids. A dye tracer test showed that the flow was uniform and indicated that four hours was sufficient to rinse the channel free of residual solution. Samples from the outflow were analyzed for colloids to verify that the four-hour rinse was sufficient to remove all unattached colloids.

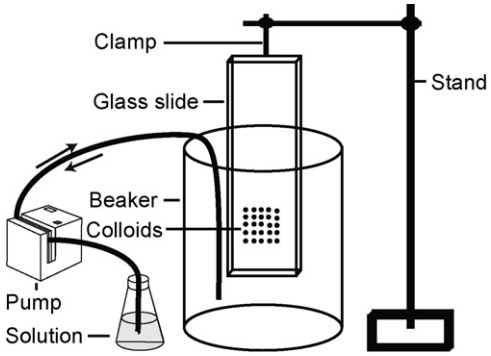

Fig. 1. Setup for the moving liquid–gas interface experiments (arrows pointing to the right and left indicate the directions of flow during up- and downward movement of the liquid–gas interface, respectively).

After the four-hour rinse, the flow was stopped and the solution in the channel was evaporated at room temperature. The deposition experiments were done in a laminar air-flow chamber (Laminar Airflow Cabinets, NuAire Corp., Plymouth, MN) to prevent contamination by dust. After air-drying, we cleaned the bottom side of the glass slide with moistened Kimwipe tissue (Kimberly-Clark Corp., Roswell, GA), so that only the upper side of the slide contained deposited colloids.

We measured the air–water–solid contact angle for the glass slides with the sessile drop method (DSA 100, Krüss, Hamburg, Germany), and the ζ-potentials by crushing the glass in a mortar with a pestle to produce colloidal-sized fragments that were then analyzed by dynamic light scattering for their electrophoretic mobility (ZetaSizer 3000HSa, Malvern Instruments Ltd., Malvern, UK).

2.4. Confocal microscopy and image analysis

We visualized the colloids on the microscope slide with a laser scanning confocal microscope (Axiovert 200M equipped with LSM 510 META, Carl Zeiss Jena GmbH, Germany). We used a 10× magnification lens for visualization and image capturing, which was sufficient to see single colloidal particles. Cross marks were made with a diamond-point pen on the microscope slide, so that the slide always could be positioned at the same locations on the confocal microscope. We selected 18 locations on each slide for imaging, with each image covering an area of 900 µm × 900 µm.

The images captured by the confocal microscope were analyzed using the ImageJ software [17]. With ImageJ, we determined the number of individual particles as well as the percentage of area covered by particles on each image. For the data analysis, we used the number of particles; the area of the individual particles was not constant because some particles were not exactly in the focal plane of the microscope, and therefore individual particles appeared in non-uniform size.

2.5. Air–water interface displacement experiments

After the colloids were deposited and the glass slides were air dry, the slides were mounted vertically into a 200 mL glass beaker using a clamp and a laboratory stand (Fig. 1). A colloid-free aqueous solution of the same chemical composition as the deposition solution was then pumped into the beaker at a specific flow rate of 60 mL/h with a peristaltic pump (Ismatec IP4, Glattburg, Switzerland). This caused the water level in the beaker to rise with a constant velocity of 4 cm/h. As the water level rose, the air–water interface moved over the colloid-deposited glass slide. When the solution reached the top of the beaker, we continued the pumping for 10 min to allow the beaker to overflow. This ensured that the colloids that were attached to the air–water interface were flushed away from the air–water interface. Then, the water was pumped out of the beaker at the same flow rate as the inflow rate. When the beaker was empty, the slide was air dried, and removed for confocal microscopy and image analysis. After image analysis, the slide was remounted into the beaker, and another air–water interface was passed over the slide at the same flow rate as described above. This procedure was repeated in total three times, so that six liquid–gas interfaces (three upward, three downward) moved over each slide.

The effect of the interface velocity on colloid removal was tested by varying the pump rate of the solution inside the beaker. The interfacial velocities were 0.4, 0.8, 4, 40, and 400 cm/h. These velocities are considerably smaller than those used by Gomez-Suarez and co-workers [2,4], whose velocities ranged from 700 to 5000 cm/h. We chose our velocities to be more typical for saturated and unsaturated flow in soils [18]. For the velocity experiments, we used amino- and carboxylate-modified colloids to represent positive and negative surface charges. Only one up and down movement of the interface was used, because the multiple passage experiments showed that most colloids detached during the first two interface movements (see Section 4.1).

2.6. Statistical analysis

The experimental data were analyzed by a one-way ANOVA and Tukey pair-wise comparison to determine statistical differences among experimental treatments [19]. A 95% confidence level was chosen for these statistical tests.

3. Theory

3.1. DLVO forces

The DLVO profiles for the colloids and their interaction with the glass surface were calculated according to [20]:

$$\Delta G_{\mathrm{el}} = 64\pi\epsilon R\left(\frac{kT}{ze}\right)^2 \times\left[\tanh\left(\frac{ze\psi_{0,1}}{4kT}\right)\right]\left[\tanh\left(\frac{ze\psi_{0,2}}{4kT}\right)\right]\exp(-\kappa h), \tag{1}$$

where ΔG_{el} is the electrostatic interaction energy, ϵ is the dielectric permittivity of the medium, R is the radius of the colloids, k is the Boltzmann constant, T is the absolute temperature; z is the ion valence, e is the electron charge, $\psi_{0,1}$ and $\psi_{0,2}$ are surface potential of the colloids and the glass slide, respectively, which are taken as the colloid and the glass ζ-potentials, h is the separation distance, κ is the inverse Debye–Hückel length,

$$\kappa = \sqrt{\frac{e^2\sum n_j z_j^2}{\epsilon kT}},$$

where n_j is the number concentration of the ions in solution, and z_j is the ion valence.

The van der Waals interaction energy was calculated by [21]:

$$\Delta G_{\mathrm{vdw}} = -\frac{AR}{6h}\left[1-\frac{5.32h}{\lambda_0}\ln\left(1+\frac{\lambda_0}{5.32h}\right)\right], \tag{2}$$

where A is the effective Hamaker constant of colloid–water–glass system, and λ_0 is a characteristic length of 100 nm. The effective Hamaker constant ($A = A_{123}$) was calculated using individual Hamaker constants of colloid, water, and glass [22].

$$A_{123} = (\sqrt{A_{11}} - \sqrt{A_{22}})(\sqrt{A_{33}} - \sqrt{A_{22}}), \tag{3}$$

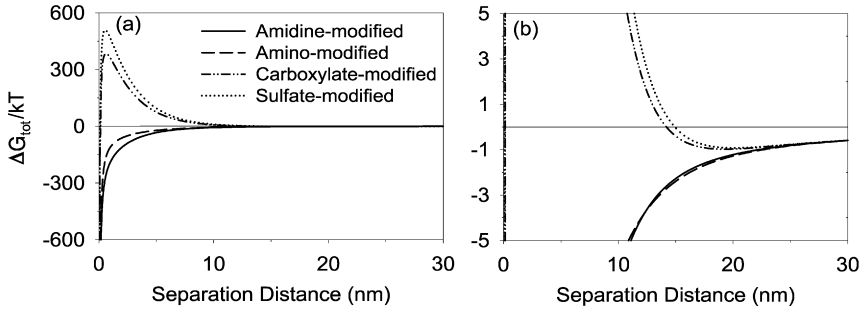

Fig. 2. Normalized DLVO energy profiles for different colloids interacting with glass surface for the experimental conditions used in our experiments: (a) full view and (b) detailed view of secondary minima.

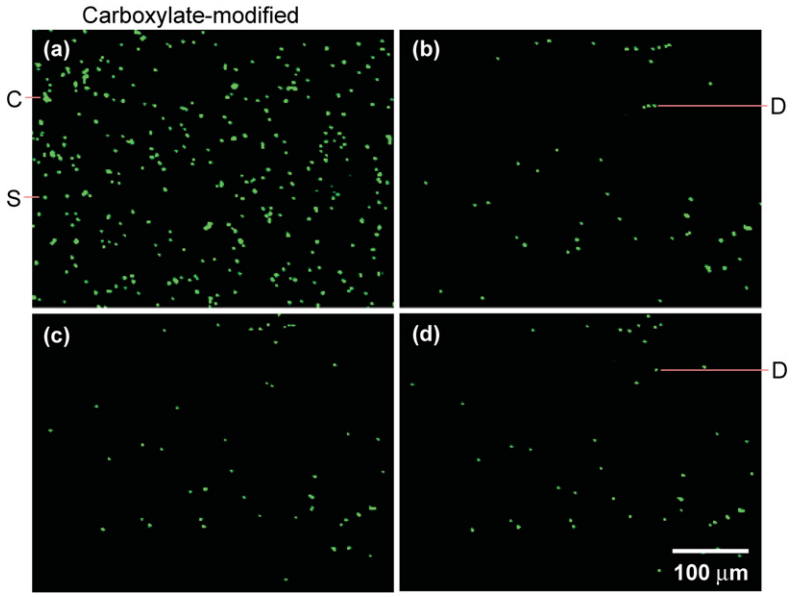

Fig. 3. Detachment of carboxylate-modified microspheres from glass slide after moving the liquid–gas interface: (a) no interface movement, (b) 2 interface movements, (c) 4 interface movements, and (d) 6 interface movements. S: single colloidal particle, C: colloid cluster, and D: displaced colloidal particle.

where A_{11} is the Hamaker constant of the colloids, A_{22} is the Hamaker constant of the fluid, and A_{33} is the Hamaker constant of the glass.

Finally, the total DLVO forces were calculated as:

$$F_{\mathrm{DLVO}} = \frac{\mathrm{d}}{\mathrm{d}h}(\Delta G_{\mathrm{tot}}) = \frac{\mathrm{d}}{\mathrm{d}h}(\Delta G_{\mathrm{el}} + \Delta G_{\mathrm{vdw}}). \tag{4}$$

Some of the parameters for the DLVO calculations are shown in Table 1, and the Hamaker constant was chosen as that for a polystyrene–water–glass system (polystyrene: $A_{11} = 6.6 \times 10^{-20}$ J, water: $A_{22} = 3.7 \times 10^{-20}$ J, glass: $A_{33} = 6.34 \times 10^{-20}$ J; all data taken from Israelachvili [23]; the combined Hamaker constant calculated with Eq. (3) is $A_{123} = 3.84 \times 10^{-21}$ J).

The results of the DLVO calculations for the different colloids in the chosen solutions are shown in Fig. 2. The DLVO calculations showed favorable attachment for amidine- and amino-modified microspheres i.e., a strong attractive force between colloids and the glass surface; and unfavorable attachment for carboxylate- and sulfate-modified microspheres i.e., colloids attached to the glass surface in the secondary energy minimum. The repulsive peaks under the unfavorable conditions were $>400kT$, and the attractive secondary energy minima were about $-1kT$.

3.2. Surface tension forces

The total force exerted by a moving liquid–gas interface on a colloidal particle is the sum of gravity, buoyancy, and interfacial forces. However, the gravity and buoyancy forces can be neglected for small particles with radii <500 μm [6,11,12,24]. In our experimental setup, when the liquid–gas interface moves in upward direction over the vertically mounted glass slide, the horizontal component of surface tension force (F_γ) is the detachment force (F_{det}) which is opposed by the DLVO force (F_{att}). The detachment force (the maximum horizontal surface tension force) can be calculated by [3,6,11,24]:

$$F_{\mathrm{det}} = 2\pi R\gamma \sin^2\left(\frac{\theta}{2}\right)\cos\alpha, \tag{5}$$

where R is the radius of the particle, γ is the surface tension of liquid, and θ and α are the contact angles for colloids and the glass slide, respectively.

4. Results and discussion

4.1. Colloid removal during the passage of an air–water interface

Fig. 3 shows the images captured by confocal microscopy for the carboxylate-modified colloids before and after passages of the air–water interface for an interface velocity of 4 cm/h. The images represent typical patterns out of the 900 μm × 900 μm area of the 18 images taken. Only the images for carboxylate-modified colloids are presented here, the results for the other types of colloids were qualitatively similar. Image (a) represents the initial pattern of col-

Table 2
Percent colloids attached to the glass slide after movement of liquid–gas interface

Colloids	Number of liquid–gas interfaces passing over deposited colloids			
	0	2	4	6
	Percent of colloids remaining deposited on the glass slide (%)			
Amidine-modified	100 Aa	7.1 ± 2.2 Ab	6.1 ± 2.9 Ab	6.1 ± 3.1 Ab
Amino-modified	100 Aa	35.3 ± 3.9 Bb	33.6 ± 3.9 Bb	32.9 ± 3.8 Bb
Carboxylate-modified	100 Aa	14.6 ± 4.8 Cb	10.5 ± 3.2 Cb	10.7 ± 2.9 Cb
Sulfate-modified	100 Aa	6.8 ± 1.1 Ab	5.5 ± 0.5 Ab	4.6 ± 1.0 Ab

Note. Data are means and standard deviations from 18 measurements. Different capital letters (A, B, and C) denote statistical differences column-wise; and different lower cases (a and b) denote statistical differences row-wise; both at a significance level of 5%.

loid deposition without passage of an air–water interface. These initial patterns show that the colloids were mostly deposited as single particles (indicated by the letter "S" in the figures); but at some locations, colloids were deposited as clusters of a few particles (indicated by the letter "C"). These clusters were examined by higher-resolution confocal microscopy and found to be single layers, i.e., colloids were deposited on the glass slide in close proximity, but without touching each other. At the resolution of the images shown in Fig. 3a, these clusters appear as single, large dots.

After the passage of the air–water interface over the slides, we observed that a considerable amount of colloids was removed (Fig. 3). Quantitative image analyses showed that the majority of the colloids were removed after the first two interface movements, and subsequent interface movements did not cause much additional detachment of colloids. There was no significant increase in the amount of colloid detachment after two passages (one upward and one downward) (Table 2).

Gomez-Suarez and co-workers [2,4] reported a nearly linear relationship between the number of air-bubbles passed over deposited colloids at a speed of 5000 cm/h and the amount of colloid detachment. This observation was explained by the authors by a limited capacity of air-bubbles to remove colloids. The authors emphasized that the speed of the air-bubble movement played an important role in detachment of colloids; the lower the speed of the air-bubbles, the less the impact of the number of air-bubbles on colloid detachment. At a lower speed (700 cm/h), however, they also observed that most colloids were detached by a single air-bubble [2]. The lower the velocity, the longer the contact time for bubble-colloid interaction is, and the more particles attach to the air-bubble [10]. In our experiments, the speed of the air–water interface was several orders of magnitude lower (4 cm/h) than the speed used by Gomez-Suarez and co-workers [2,4] (700 to 5000 cm/h). The contact time in our experiments was therefore so long, that most colloids attached to the air–water interface in the first two passages of the interface, and subsequent interface movements had an insignificant effect (Table 2). Furthermore, the air–water interface in our experiment was so large compared to the number and surface area of the colloids, that no limitation of the carrying capacity of the interface for colloids is expected.

The first two passages of the air–water interface had a dominant effect on colloid detachment, no matter whether the colloids were attached under favorable or unfavorable conditions. As Fig. 2 shows, colloids deposited in the secondary minimum had a separation from the glass plate of about 18 nm. However, when the water on the slide evaporated, the water-film became smaller and smaller, and ultimately, the capillary forces, forming between the colloids and the glass surface, pulled the particles closer to the glass surface. The capillary forces exerted by a drying liquid film for our experimental system were in the order of 10^{-7} N, as calculated using the Young–Laplace equation. These forces were a few orders of magnitude stronger than the repulsive DLVO forces at the energy barrier of the unfavorable attachment ($\approx 10^{-14}$ N). It is therefore likely that during drying, some colloids were pulled over the repulsive energy barrier and moved into the primary energy minimum. The colloids remaining in the secondary minimum and a fraction of the colloids in the primary minimum were detached after the first two passages of the air–water interface. The colloids that were attached strongly enough to resist detachment by the first two air–water interface passages remained attached even after subsequent interface movements.

We observed that some of the colloids on the glass slide were displaced from the original position on the slides after passage of the liquid–gas interface (Fig. 3, the displaced particles are denoted by the letter "D"). The displacement was likely caused by the vertical component of the surface tension force. We believe that these particles were translocated along the glass slide without detaching from the slide. It is unlikely that particles first detached from the solid–water interface and attached to the air–water interface, and then reattached to the solid–water interface, because the forces at the air–water interface are usually so strong that the attachment to the air–water interface can be considered irreversible in a system like ours [25,26].

The hydrophobic colloids (amidine- and sulfate-modified) detached in larger amounts than did the hydrophilic colloids (amino- and carboxylate-modified) (Table 2). There was a significant difference in the amount of colloid remaining attached to the glass slides after air–water interface movements between the hydrophobic and hydrophilic colloids (Table 2). Our experimental data are consistent with force considerations, which show that the detachment force was about 10^{-7} N for hydrophobic and 10^{-8} N for hydrophilic colloids [Eq. (5)].

We found significantly less detachment of the hydrophilic, positively-charged (amino-modified) colloids than of the hydrophilic, negatively-charged colloids (carboxylate-modified) (Table 2). The positively-charged colloids were deposited in the primary energy minimum, and had a stronger attachment to the solid–water interface than the negatively-charged colloids. Our experimental observations are therefore in qualitative agreement with theoretical expectations. Similar observations were reported by Gomez-Suarez and co-workers [4], who found more removal of negatively-charged polystyrene colloids from a negatively-charged dimethyldichlorosilane (DDS) coated glass surface than from a positively-charged 3-(2-aminoethylamino)propyldimethoxysilane (APTS) coated glass surface [2].

For the hydrophobic colloids, however, no significant difference in detachment between positively- and negatively-charged colloids (amidine- and sulfate-modified) was observed (Table 2). Although the positively-charged colloids were attached stronger than the negatively-charged colloids to the solid–water interface, no differences in their removal was found. The force calculations (discussed in Section 4.2 below) indicate that the detachment forces dominated the attachment forces by orders of magnitude, and consequently were overshadowing the effect of the attachment conditions (favorable vs unfavorable).

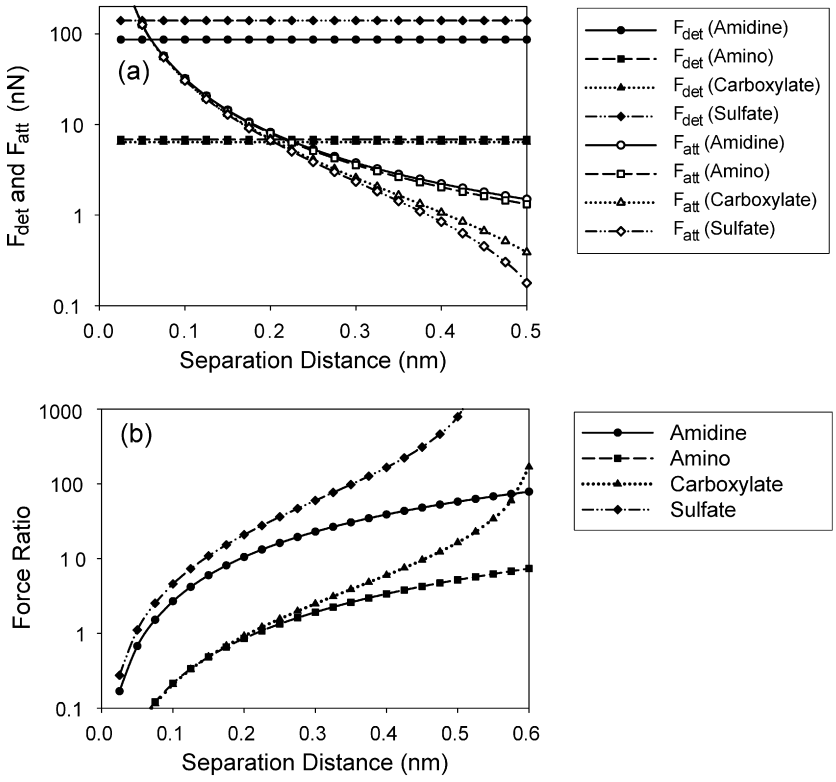

Fig. 4. (a) Detachment and attachment forces and (b) ratio of detachment and attachment force, in relation to separation distance for the different colloids.

4.2. Force balance and comparison with experimental results

The attachment forces [Eq. (4)] and the detachment forces [Eq. (5)] as a function of separation distance for individual colloids with a glass surface are shown in Fig. 4a. The detachment forces dominated the attachment forces, except at small separation distances, and were much stronger for hydrophobic colloids than for hydrophilic colloids. According to the force calculations, hydrophobic colloids should have been completely removed from the glass slides, as the detachment forces were much larger than the attachment forces. We assume the closest approach distance for the solid–water interface interaction is 0.3 nm [27]. However, about 5–10% of the colloids remained attached to the glass slides, even after multiple passages of the air–water interface. We speculate that the fraction of non-detachable colloids was either closer to the interface as expected, or that other reasons (e.g., surface roughness, variability in hydrophobicity) caused either stronger attraction or weaker detachment than expected. It may also be possible that the liquid–gas interface jumped over some particles without making a three-phase contact line. Incomplete detachment has also observed by others [28], and has been attributed to the statistical nature of the detachment process.

The hydrophobic colloids (amidine-modified and sulfate-modified) experienced an about 10-times stronger detachment force than the hydrophilic colloids (amino-modified and carboxylate-modified), and consequently more hydrophobic colloids should be removed by a passage of an air–water interface, as corroborated by our experiments. The prominence of the detachment force for hydrophobic colloids may also explain why there was so little difference in detachment between the hydrophobic colloids (amidine-modified and sulfate-modified).

The theoretical sequence of colloid removal from the glass slides is shown in Fig. 4b, where the ratio between detachment and attachment forces is plotted. The hydrophobic, negatively-charged sulfate-modified colloids should be removed the most based on theory (Fig. 4b), and the experimental data are in qualitative agreement with this (Table 2). The hydrophilic, positively-charged amino-modified colloids should be removed the least based on theory, and the experiments corroborate this. In general, the sequence of colloid detachment observed experimentally (Table 2) is according to theory (Fig. 4b): the detachment followed the sequence sulfate > amidine > carboxylate > amino.

The detachment force strongly depends on the value of the contact angles θ and α. Both of these angles are hysteretic, i.e., we expect that during the upward movement of the interface, the advancing contact angles are the relevant angles, and during downward movement, the receding contact angles are relevant. This would cause the detachment force [Eq. (5)] to be larger during upward movement than during downward movement. Based on this, we would expect that most colloids were removed during the upward movement of the interface. We do not have experimental data to confirm this hypothesis, as we only have colloid removal data for a complete (up- and downward) sequence.

4.3. Effect of air–water interface velocity

Fig. 5 shows the amounts of colloids remaining at the glass slides after passage of two air–water interfaces at different velocities. The data generally indicate increased removal of colloids with decreasing velocity of the air–water interface. The positively-charged colloids (amino-modified) were more sensitive to interface velocity than the negatively-charged colloids. However, the relationship between detachment and velocity was not linear as reported by Gomez-Suarez and co-workers [2,4]. The velocity effect observed by Gomez-Suarez and co-workers was explained by the thickening of the liquid film between air-bubbles and the solid-liquid interface with increased velocity, leading to a decrease in the detachment force. In our experiments, the solid surface was initially dry when the air–water interface passed over the solid surface, so that the effect of the interface velocity can not be due to film thinning/thickening between the solid surface and the

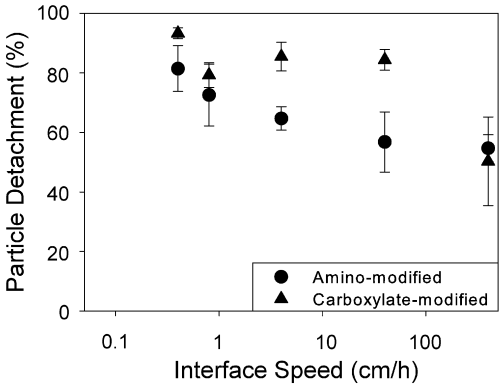

Fig. 5. Detachment of colloids from solid surfaces as a function of air–water interface velocity. Symbols are means and bars represent ± one standard deviation.

air–water interface, but rather due do film thinning/thickening between colloids and the air–water interface. Viscous forces are generally too small to be of relevance [4].

The removal of colloids from the solid surface by a moving air–water interface is considered to comprise of three different steps: interception of the particle, attachment or thinning of the liquid film in between the colloid and the air–water interface, and stabilization of the colloid on the air–water interface [2,10]. The detachment probability (P_d) can be defined as [10]:

$$P_d = P_i \times P_a \times P_s, \tag{6}$$

where P_i is the interception probability, P_a the attachment probability, and P_s the stability probability. In our experiments, the interception probability was $P_i = 1$, because the air–water interface was forced to intercept all the particles, i.e., we made the air–water interface move over attached colloids by raising the water level in the beaker. The attachment probability depended on velocity of the air–water interface. The colloidal particles attached to the air–water interface only if the contact time was larger than the induction time. The induction time is the time for the liquid film between the particle and the air–water interface to thin and form a three-phase contact line. Therefore, the detachment of colloids from the solid surfaces only happens if the velocity of the air–water interface is low enough that the contact time with the colloid is greater than the induction time. We consider the stability probability to be $P_s = 1$, because of the irreversibility of the colloid attachment to the air–water interface, i.e., once the particle attached to the interface, it remained there.

We therefore interpret the velocity effects seen in Fig. 5 as a consequence of a changing attachment probability P_a. The velocities in our experiments (0.4 to 400 cm/h) were smaller than those used by Gomez-Suarez and co-workers [2,28] in their air-bubble experiments (700 to 5000 cm/h). The attachment probability P_a in our experiments should therefore be greater than in the Gomez-Suarez experiments, and the linear relationship between detachment and velocity may not hold for our slow velocities.

5. Implications

In subsurface systems, like soils and sediments, moving air–water interfaces are common, e.g., during infiltration and drainage of water, air and water displace each other in continuous cycles. Such moving air–water interfaces have a profound effect on detachment of colloids from surfaces. As our experiments with polystyrene microspheres showed, colloids can be mobilized effectively when an air–water interface moves over an air-dried surface, suggesting that during infiltration into a dry soil, colloids can readily be captured at the air–water interface and moved along with the displacement of the air–water interface. Even when the soil is not air-dry, but rather contains residual moisture or has a higher water content, an infiltrating or draining water front will be able to remove colloids that are attached to the stationary mineral surfaces, as long as the colloids come into contact with the moving air–water interface.

Our experiments further suggest that the majority of the colloids will be removed by the first air–water interface movements, which helps to explain experimental findings on colloid mobilization from porous media reported in literature. Several authors have shown that during infiltration, the majority of the colloids is mobilized with the first of a multiple infiltration sequence [13,29–32] or at that the largest colloid concentrations were observed at the beginning of elution curves [33,34]. We provide a mechanistic interpretation for these findings; other factors also contribute to colloid mobilization in porous media, but at least, the air–water interface contribution can be substantial as shown by our experiments. Our experiments reported here demonstrate clearly the important role of the air–water interface for colloid mobilization and transport in porous media.

The strong attachment of colloidal particles to liquid–gas interfaces, leading to removal of stationary surfaces, offers opportunities for management of subsurface systems in terms of flow and transport. Infiltration fronts in soils can be readily generated by flooding, for instance, and colloids may be effectively "washed" out of a soil profile.

Supplementary material

The online version of this article contains additional supplementary material.

Please visit DOI: 10.1016/j.jcis.2008.07.030.

References

[1] J. Noordmans, P.J. Wit, H.C. van der Mei, H.J. Busscher, J. Adhes. Sci. Technol. 11 (1997) 957.
[2] C. Gomez-Suarez, J. Noordmans, H.C. van der Mei, H.J. Busscher, Phys. Chem. Chem. Phys 1 (1999) 4423.
[3] A.F.M. Leenaars, S.B.G. O'Brien, Philips J. Res. 44 (1989) 183.
[4] C. Gomez-Suarez, J. Noordmans, H.C. van der Mei, H.J. Busscher, Langmuir 15 (1999) 5123.
[5] C. Gomez-Suarez, J. Noordmans, H.C. van der Mei, H.J. Busscher, Colloids Surf. 186 (2001) 211.
[6] M. Preuss, H. Butt, Langmuir 14 (1998) 3164.
[7] G. Gillies, M. Kappl, H. Butt, Adv. Colloid Interface Sci. 114 (2005) 165.
[8] D.J. Johnson, N.J. Miles, N. Hilal, Adv. Colloid Interface Sci. 127 (2006) 67.
[9] J. Ralston, S.S. Dukhin, Colloids Surf. 151 (1999) 3.
[10] Z. Dai, D. Fornasiero, J. Ralston, J. Colloid Interface Sci. 217 (1999) 70.
[11] O. Pitois, X. Chateau, Langmuir 18 (2002) 9751.
[12] P. Sharma, H. Abdou, M. Flury, Vadose Zone J. 7 (2008) 930.
[13] J. Shang, M. Flury, G. Chen, J. Zhuang, Water Resour. Res. 44 (2008) W06411, doi:10.1029/2007WR006516.
[14] J.M. Wan, J.L. Wilson, Water Resour. Res. 30 (1994) 11.
[15] A.A. Keller, M. Auset, Adv. Water Resour. 30 (2007) 1392.
[16] S. Sirivithayapakorn, A. Keller, Water Resour. Res. 39 (2003) 1346, doi:10.1029/2003WR002487.
[17] NIH, ImageJ, A public domain Java image processing program from National Institute of Healths, on-line at http://rsb.info.nih.gov/ij, accessed in August, 2007.
[18] A. Klute, C. Dirksen, Hydraulic conductivity and diffusivity: Laboratory methods, in: A. Klute (Ed.), Methods of Soil Analysis, Part 1, Physical and Mineralogical Methods, second ed., American Society of Agronomy, Madison, WI, 1986, pp. 687–734.
[19] SAS Institute Inc., SAS/STAT User's Guide, Vers. 6, vol. 2, fourth ed., SAS Institute Inc., Cary, NC, 1990.
[20] J. Gregory, J. Colloid Interface Sci. 51 (1975) 44.
[21] J. Gregory, J. Colloid Interface Sci. 83 (1981) 138.
[22] P.C. Hiemenz, R. Rajagopalan, Principles of Colloid and Surface Chemistry, third ed., Marcel Dekker, New York, 1997.
[23] J. Israelachvili, Intermolecular and Surface Forces, Academic Press, London, 1992.
[24] A. Scheludko, B.V. Toshev, D.T. Bojadjiev, J. Chem. Soc. Faraday Trans. I 72 (1976) 2815.
[25] A.I. Abdel-Fattah, M.S. El-Genk, J. Colloid Interface Sci. 202 (1998) 417.

[26] A.I. Abdel-Fattah, M.S. El-Genk, Adv. Colloid Interface Sci. 78 (1998) 237.
[27] M. Elimelech, J. Gregory, X. Jia, R.A. Williams, Particle Deposition and Aggregation: Measurement, Modelling, and Simulation, Butterworth–Heinemann, Oxford, 1995.
[28] C. Gomez-Suarez, H.C. van der Mei, H.J. Busscher, J. Adhes. Sci. Technol. 14 (2000) 1527.
[29] Y.H. El-Farhan, N.M. Denovio, J.S. Herman, G.M. Hornberger, Environ. Sci. Technol. 34 (2000) 3555.
[30] J. Zhuang, J.F. McCarthy, J.S. Tyner, E. Perfect, M. Flury, Environ. Sci. Technol. 41 (2007) 3199.
[31] J.E. Saiers, J.J. Lenhart, Water Resour. Res. 39 (2003) 1019, doi:10.1029/2002WR001370.
[32] B. Gao, J.E. Saiers, J.N. Ryan, Water Resour. Res. 40 (2004) W08602, doi:10.1029/2004WR003189.
[33] O.H. Jacobsen, P. Moldrup, H. de Jonge, L.W. de Jonge, Phys. Chem. Earth 23 (1998) 159.
[34] M. Laegdsmand, L.W. de Jonge, P. Moldrup, Soil Sci. 170 (2005) 13.